

CONFIDENTIAL

Copy
RM E56118

330

N63-12532

code-1



RESEARCH MEMORANDUM

EXPERIMENTAL INVESTIGATION OF A HIGH SUBSONIC
MACH NUMBER TURBINE HAVING HIGH ROTOR
BLADE SUCTION-SURFACE DIFFUSION

By William J. Nusbaum and Cavour H. Hauser

Lewis Flight Propulsion Laboratory
Cleveland, Ohio

CLASSIFICATION CHANGED TO
UNCLASSIFIED
EXEMPT NARA LIST 1, 2, 3, 4, 5, 6, 7, 8, 9, 10, 11, 12, 13, 14, 15, 16, 17, 18, 19, 20, 21, 22, 23, 24, 25, 26, 27, 28, 29, 30, 31, 32, 33, 34, 35, 36, 37, 38, 39, 40, 41, 42, 43, 44, 45, 46, 47, 48, 49, 50, 51, 52, 53, 54, 55, 56, 57, 58, 59, 60, 61, 62, 63, 64, 65, 66, 67, 68, 69, 70, 71, 72, 73, 74, 75, 76, 77, 78, 79, 80, 81, 82, 83, 84, 85, 86, 87, 88, 89, 90, 91, 92, 93, 94, 95, 96, 97, 98, 99, 100

CLASSIFIED DOCUMENT

This material contains information affecting the National Defense of the United States within the meaning of the espionage laws, Title 18, U.S.C., Secs. 793 and 794, the transmission or revelation of which in any manner to an unauthorized person is prohibited by law.

NATIONAL ADVISORY COMMITTEE
FOR AERONAUTICS

WASHINGTON

November 20, 1956

CONFIDENTIAL

U.S. PRICE

XEROX

MICROFILM

\$

\$

UNCLASSIFIED

NACA RM E56I18

CONFIDENTIAL

NATIONAL ADVISORY COMMITTEE FOR AERONAUTICS

RESEARCH MEMORANDUM

EXPERIMENTAL INVESTIGATION OF A HIGH SUBSONIC MACH NUMBER TURBINE
HAVING HIGH ROTOR BLADE SUCTION-SURFACE DIFFUSION

By William J. Nusbaum and Cavour H. Hauser

SUMMARY

A high subsonic Mach number turbine with high suction-surface diffusion was investigated experimentally. The subject turbine was designed for a high weight flow per unit frontal area, a high specific work output, and a relative critical velocity ratio of 0.82 at the rotor hub inlet. At the equivalent design blade speed and work output, the brake internal efficiency based on the actual over-all total-pressure ratio was 0.871, which is only 0.004 less than the efficiency of a turbine with the same design characteristics but with higher solidity and with low diffusion on the suction surface.

The calculated value of the ratio of effective rotor blade momentum thickness to mean camber length of 0.014 is considerably greater than the value previously obtained for transonic turbines having the same average total surface diffusion parameter. These results indicate that the effective rotor blade momentum thickness depends not only on the average total surface diffusion parameter but also on the effect of changes in hub-tip radius ratio, the distribution of the surface diffusion over the blade height and between the two surfaces of the blade, and the possible variation in the velocity distribution for a given value of surface diffusion.

INTRODUCTION

In the aerodynamic design of turbine rotor blades for a given application, a compromise must be made in selecting the solidity of the blade row. A decrease in solidity has the advantage of a reduction in the sum of blade and end-wall surface areas where the boundary layer is produced. However, as the solidity of a blade row is decreased there is an increase in blade loading with a resultant increase in momentum loss per unit surface area (ref. 1). For low-reaction blade rows an increase in blade loading results in increased values of the blade surface diffusion parameters. Thus, in order that a selection of the value of solidity giving

CONFIDENTIAL

minimum over-all blade loss can be accurately made, it is necessary to establish the variation of over-all blade loss with both solidity and surface diffusion parameter.

The variation of rotor blade boundary-layer momentum-thickness parameter $\bar{\theta}_{tot}/l$ with diffusion parameter for five transonic turbine designs is presented in reference 2. These turbines were designed for high work output, having a relative inlet critical velocity ratio of unity at the hub of the rotor.

The design and over-all performance of the first of a series of high subsonic Mach number turbines having high weight flow per unit frontal area and high specific work output are presented in reference 3. This turbine is hereinafter referred to as configuration I. The subject turbine is the second in this series and is referred to herein as configuration II. The rotor hub inlet relative critical velocity ratio is 0.82 for both of these designs.

The rotor of configuration I, having 58 blades, had relatively low diffusion on the blade surfaces. It is desired to evaluate the effect of using higher values of rotor blade surface diffusion in a turbine having the same design characteristics and velocity diagrams. The purpose of the present investigation is to evaluate the performance of configuration II, which has only 40 rotor blades and considerably higher values of rotor blade suction-surface diffusion. The results of the performance investigation at equivalent design operating conditions are evaluated in terms of the ratio of effective rotor blade momentum thickness to mean camber length $\bar{\theta}_{tot}/l$ and are compared with the values for the transonic turbine rotors presented in reference 2 and with the value for the turbine rotor of configuration I (ref. 3).

SYMBOLS

a_{cr} critical velocity of sound, ft/sec

D_p pressure-surface diffusion parameter,

$$\frac{\text{Blade inlet relative velocity} - \text{Min. blade surface relative velocity}}{\text{Blade inlet relative velocity}}$$

D_s suction-surface diffusion parameter,

$$\frac{\text{Max. blade surface relative velocity} - \text{Blade outlet relative velocity}}{\text{Max. blade surface relative velocity}}$$

D_{tot} sum of suction- and pressure-surface diffusion parameters, $D_p + D_s$

$\Delta h'$ specific work output, Btu/lb

NOT REPRODUCED
 CONFIDENTIAL

UNCLASSIFIED

- l length of mean camber line, ft
 p absolute pressure, lb/sq ft
 r radius, ft
 U blade velocity, ft/sec
 V absolute gas velocity, ft/sec
 W relative gas velocity, ft/sec
 w weight flow, lb/sec
 γ ratio of specific heats
 γ° blade-chord angle, angle between blade chord and axial direction, deg
 δ ratio of inlet-air total pressure to NACA standard sea-level pressure, p_1/p^*

ϵ function of $\gamma, \frac{\gamma^*}{\gamma} \left[\frac{\left(\frac{\gamma + 1}{2} \right)^{\frac{\gamma}{\gamma - 1}}}{\left(\frac{\gamma^* + 1}{2} \right)^{\frac{\gamma^*}{\gamma^* - 1}}} \right]$

- η brake internal efficiency, defined as ratio of turbine work based on torque, weight flow, and speed measurements to ideal work based on inlet total temperature and inlet and outlet total pressures, both defined as sum of static pressure and pressure corresponding to gas velocity
 η_x brake internal rating efficiency, defined as ratio of turbine work based on torque, weight flow, and speed measurements to ideal work based on inlet total temperature and inlet and outlet axial total pressures, both defined as sum of static pressure and pressure corresponding to axial component of velocity
 θ_{cr} squared ratio of critical velocity at turbine inlet to critical velocity at NACA standard sea-level temperature, $(a'_{cr,1}/a_{cr}^*)^2$
 $\bar{\theta}_{tot}$ effective rotor blade momentum thickness based on turbine over-all performance, ft

CONFIDENTIAL

ψ coefficient of aerodynamic loading

Subscripts:

- m mean
- t tip
- u tangential
- x axial
- 1 station upstream of stator
- 2 station at trailing edge of stator
- 3 station at free-stream condition between stator and rotor
- 4 station at trailing edge of rotor
- 5 station downstream of rotor

Superscripts:

- * NACA standard condition
- ' stagnation state
- " relative stagnation state

TURBINE DESIGN

Design Requirements

The design requirements of the subject 14-inch cold-air turbine are the same as those for configuration I (ref. 3) and are as follows:

- Equivalent specific work output, $\Delta h' / \theta_{cr}$, Btu/lb 20.60
- Equivalent weight flow, $\frac{\epsilon w \sqrt{\theta_{cr}}}{\delta}$, lb/sec 16.10
- Equivalent blade tip speed, $U_t / \sqrt{\theta_{cr}}$, ft/sec 720

Velocity Diagrams

The stator of the subject turbine is the same as that of turbine configuration I. The design velocity diagrams (fig. 1) are also the

UNCLASSIFIED

same at stations 3 and 5. However, at station 4 just upstream of the rotor blade trailing edge the velocity diagrams are slightly different from those of configuration I, because the subject turbine rotor has about 2 percent less trailing-edge blockage than the turbine rotor of configuration I. The assumptions of reference 3 used in obtaining the rotor design velocity diagrams are

- (1) Free-vortex flow
- (2) Simplified radial equilibrium
- (3) Design value of over-all adiabatic efficiency of 0.90
- (4) No change in the tangential velocity component between stations 4 and 5
- (5) No loss in total pressure between stations 4 and 5

Rotor Blade Design Procedure

The design procedure is the same as that used for the design of the rotor blades of configuration I as described in reference 3, with the following two exceptions:

(1) The blade chord at the mean section was chosen arbitrarily. The number of blades was then determined by applying the criterion of reference 4 (using a coefficient of aerodynamic loading ψ of 1.0 rather than 0.80 as in ref. 3) at the blade mean section.

(2) A maximum allowable value of the suction-surface diffusion parameter D_s was set at 0.31 as compared with the design value of 0.12 for the rotor of configuration I.

Table I gives the coordinates of the final blade at the hub, mean, and tip sections. A photograph of the turbine rotor is presented in figure 2.

Discussion of Rotor Blade Design

The rotor blade profiles forming the flow passages at the hub, mean, and tip sections are shown in figure 3. The axial chord increases from hub to tip, being about 27 percent greater at the tip than at the hub. The resulting solidities are 2.1, 1.8, and 1.8 at the hub, mean, and tip sections, respectively. The turbine rotor of configuration I has solidities at hub, mean, and tip sections of 2.8, 2.2, and 2.0,

CONFIDENTIAL

respectively. Thus, the solidity at the mean section of the subject turbine rotor is about 18 percent less than that of the turbine rotor of configuration I. It may be noted in figure 3 that the three-dimensional design procedure resulted in a channel that is divergent from inlet to exit at the hub section and convergent at the tip section.

The design midchannel and surface velocity distributions at the hub, mean, and tip sections of the rotor are plotted in figure 4. The corresponding values of the surface diffusion parameters along with those for the rotor of configuration I are given in table II. A comparison of the values for the two turbines shows approximately equal values on the pressure surface. On the suction surface, however, values of the surface diffusion parameter for the subject turbine are considerably greater than those for the rotor of configuration I. The maximum difference is at the hub section, where the subject turbine has a value of 0.31 as compared with a value of zero for the turbine rotor of configuration I. Also, the average value of the total diffusion parameter for the subject turbine is approximately twice that for the turbine of configuration I.

APPARATUS, INSTRUMENTATION, AND TEST PROCEDURE

The apparatus, instrumentation, test procedure, and method of calculating the performance parameters are the same as those described in reference 3. The over-all performance data were taken at nominal values of total-pressure ratio p_1'/p_5' from 1.3 to the maximum obtainable (about 2.3), while the wheel speed was varied from 60 to 110 percent of equivalent design speed in 5-percent intervals. The absolute inlet total pressure was set at 50 inches of mercury (24.6 lb/sq in. abs), and the inlet total temperature was about 80° F.

RESULTS AND DISCUSSION

The performance map of the subject turbine based on the actual over-all total-pressure ratio p_1/p_5 is presented in figure 5(a). The equivalent specific work output $\Delta h'/\theta_{cr}$ is plotted against the weight flow - mean blade speed parameter $\epsilon wU_m/\delta$, with the actual total-pressure ratio, percent equivalent design blade speed, and brake internal efficiency as parameters. The efficiency at the point of equivalent design specific work output and blade speed is 0.871, which is only 0.004 less than the efficiency for configuration I at this point. The maximum efficiency is 0.876, and it occurs at a blade speed about 5 percent greater than the design value. The efficiency is greater than 0.86 over a large portion of the map.

UNCLASSIFIED

The performance map of the turbine based on the axial over-all total-pressure ratio $p_1/p_{5,x}$ is presented in figure 5(b). The efficiency at the point of equivalent design specific work output and blade speed is 0.870, indicating that the energy of the exit-whirl velocity component $V_{u,5}$ is negligible at this point.

The variation of the static pressure measured on the annulus walls downstream of the stator and rotor blades (stations 3 and 5) with the actual over-all total-pressure ratio at equivalent design blade speed is presented in figure 6(a). At station 5, downstream of the rotor, the average of hub and tip values of static pressure is presented because there is little variation in static pressure over the blade height. The variation of weight flow is shown in figure 6(b). As was the case for configuration I, figure 6(a) shows that there is a pressure rise across the rotor hub from stations 3 to 5 for total-pressure ratios up to about 2.16, where the rotor blade limiting-loading condition is approached. The rotor blades are choked at a total-pressure ratio of about 2.10.

The ratio of effective rotor blade momentum thickness to mean camber length $\bar{\theta}_{tot}/l$ for the subject turbine was calculated by the method of reference 2 and corrected for Reynolds number by equation (5) of reference 1 using the Reynolds number for the transonic turbines (ref. 2) as a reference value. The calculated value of 0.014 is compared with the values obtained for configuration I (ref. 3) and the six transonic turbines (ref. 2) in figure 7. The subject rotor blade has a considerably higher value of the parameter $\bar{\theta}_{tot}/l$ than the transonic turbine rotor blades having the same average total surface diffusion parameter. A number of factors may be cited to account for this difference:

(1) It is probable that an improved velocity distribution on the blade surfaces would reduce the over-all blade losses for the same value of total surface diffusion parameter D_{tot} . In particular, at the hub and mean blade sections the suction-surface diffusion parameters are considerably higher than those on the pressure surface. If the greater portion of the total diffusion required to obtain the blade loading were to occur near the leading edge on the pressure surface of the blade where the boundary layer is thin, the over-all losses through the blade row would probably be reduced. Improvement might also be obtained if the blade were more uniformly loaded along the chord length at the mean and tip sections. At these sections the portion of the blade near the trailing edge is rather lightly loaded.

(2) The calculation of the parameter $\bar{\theta}_{tot}/l$ is based on the over-all turbine efficiency and therefore includes the effects of loss caused by secondary flow in the turbine rotor. It is possible that the adverse effects of secondary flow in the rotor blades may be more pronounced in

CONFIDENTIAL

the subject turbine and configuration I than in the transonic turbines. Because of the lower hub-tip radius ratio (0.60 as compared with 0.70 for the transonic turbines) the variations in the flow conditions over the blade height may be correspondingly greater.

(3) There is a greater variation in the value of the total diffusion parameter D_{tot} over the blade height (table II) than there is for the transonic turbines. This large variation may increase the adverse effects of secondary flow and, as a result, increase the over-all losses through the blade row. The effective rotor blade momentum-thickness parameter $\bar{\theta}_{tot}/l$ may, therefore, be more a function of the maximum diffusion parameter than of the average value over the blade height.

(4) The method for calculating the parameter $\bar{\theta}_{tot}/l$ is based on the assumption that the boundary layer developed on the inner and outer annulus walls is similar to that on the blade surface at the mean section. In particular, the complex boundary-layer flow in the tip-clearance region depends on the geometry of the blading at the tip section, the tip clearance, and the blade tip speed. The higher tip speed for the subject turbine as well as for configuration I probably causes higher losses in the tip-clearance region.

(5) The effective rotor blade momentum-thickness parameter is plotted as a function of the design or theoretical value of the total diffusion parameter in figure 7. The actual velocities on the blade surface may have differed sufficiently from the design values that the actual diffusion parameter on the rotor blade surface was considerably different from the value plotted.

Although the value of the effective rotor blade momentum-thickness parameter $\bar{\theta}_{tot}/l$ for the subject turbine is approximately 30 percent greater than that for the rotor of configuration I, the brake internal efficiency based on the actual over-all total-pressure ratio at the design point was only 0.004 less for the subject turbine. This comparatively small change in the brake internal efficiency in spite of the increase in effective rotor blade momentum-thickness parameter $\bar{\theta}_{tot}/l$ is attributable to the reduction in the blade surface area corresponding to the reduced solidity.

SUMMARY OF RESULTS

The over-all performance of a high subsonic Mach number turbine having high suction-surface diffusion has been presented. The following results were obtained:

U N C L A S S I F I E D

1. The brake internal efficiency based on the actual over-all total-pressure ratio at the equivalent design blade speed and specific work output was 0.871. This value is only 0.004 lower than that obtained from a turbine having the same design characteristics but with a higher value of solidity and with lower suction-surface diffusion. The efficiency based on the axial total-pressure ratio at the same point was 0.870.

2. A value of 0.014 was calculated for the ratio of effective rotor blade momentum thickness to mean camber length. This value is considerably greater than that previously obtained for transonic turbines having the same average total surface diffusion parameter. This large difference may be due to a high value of the suction-surface diffusion as compared with that on the pressure surface, a surface velocity distribution that is not the optimum, a comparatively high variation in the value of the total diffusion parameter over the blade height, and the adverse effects of secondary flow.

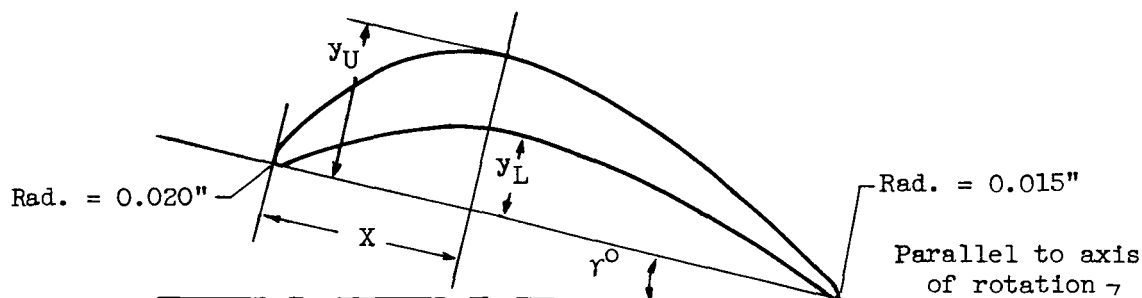
Lewis Flight Propulsion Laboratory
National Advisory Committee for Aeronautics
Cleveland, Ohio, September 19, 1956

REFERENCES

1. Miser, James W., Stewart, Warner L., and Whitney, Warren J.: Analysis of Turbomachine Viscous Losses Affected by Changes in Blade Geometry. NACA RM E56F21, 1956.
2. Stewart, Warner L., Whitney, Warren J., and Miser, James W.: Use of Effective Momentum Thickness in Describing Turbine Rotor-Blade Losses. NACA RM E56B29, 1956.
3. Hauser, Cavour H., and Nusbaum, William J.: Experimental Investigation of a High Subsonic Mach Number Turbine Having Low Rotor Suction-Surface Diffusion. NACA RM E56G25, 1956.
4. Zweifel, O.: Optimum Blade Pitch for Turbo-Machines with Special Reference to Blades of Great Curvature. The Eng. Digest, vol. 7, no. 11, Nov. 1946, pp. 358-360; cont., vol. 7, no. 12, Dec. 1946, pp. 381-383.

U N C L A S S I F I E D
CONFIDENTIAL

TABLE I. - ROTOR BLADE-SECTION COORDINATES



X, in.	Hub		Mean		Tip	
	$\gamma^0 = -6.25^\circ$		$\gamma^0 = 13.75^\circ$		$\gamma^0 = 30.8^\circ$	
	$r/r_t = 0.60$		$r/r_t = 0.80$		$r/r_t = 1.00$	
	y_L , in.	y_U , in.	y_L , in.	y_U , in.	y_L , in.	y_U , in.
0	0.020	0.020	0.020	0.020	0.020	0.020
.025	.000	.055	.001	.073	.001	.059
.100	.056	.132	.050	.189	.013	.145
.200	.124	.229	.112	.301	.031	.232
.300	.179	.314	.163	.369	.047	.289
.400	.220	.382	.200	.408	.065	.323
.500	.248	.428	.224	.428	.081	.340
.600	.264	.454	.235	.432	.094	.346
.700	.265	.458	.235	.422	.106	.346
.800	.254	.441	.228	.401	.115	.340
.900	.230	.405	.213	.372	.121	.330
1.000	.195	.349	.193	.336	.124	.316
1.100	.149	.276	.169	.293	.123	.297
1.200	.094	.190	.140	.245	.120	.274
1.300	.032	.093	.107	.193	.114	.248
1.353	.000	.037	----	----	----	----
1.368	.015	.015	----	----	----	----
1.400	----	----	.071	.138	.104	.220
1.500	----	----	.032	.080	.092	.191
1.579	----	----	.000	.033	----	----
1.594	----	----	.015	.015	----	----
1.600	----	----	----	----	.078	.162
1.700	----	----	----	----	.062	.132
1.800	----	----	----	----	.043	.099
1.900	----	----	----	----	.022	.066
2.000	----	----	----	----	.001	.032
2.004	----	----	----	----	.000	.031
2.019	----	----	----	----	.015	.015

UNCLASSIFIED

TABLE II. - COMPARISON OF ROTOR BLADE SURFACE DIFFUSION
PARAMETERS FOR SUBJECT TURBINE WITH THOSE
FOR TURBINE OF REFERENCE 3

Turbine	Section	Rotor blade surface diffusion parameter		
		Suction surface, D_s	Pressure surface, D_p	Total, D_{tot}
Configuration I (Ref. 3)	Hub	0.00	0.27	0.27
	Mean	.06	.12	.18
	Tip	.12	.06	.18
Configuration II (Subject)	Hub	0.31	0.25	0.56
	Mean	.27	.07	.34
	Tip	.15	.13	.28

CONFIDENTIAL

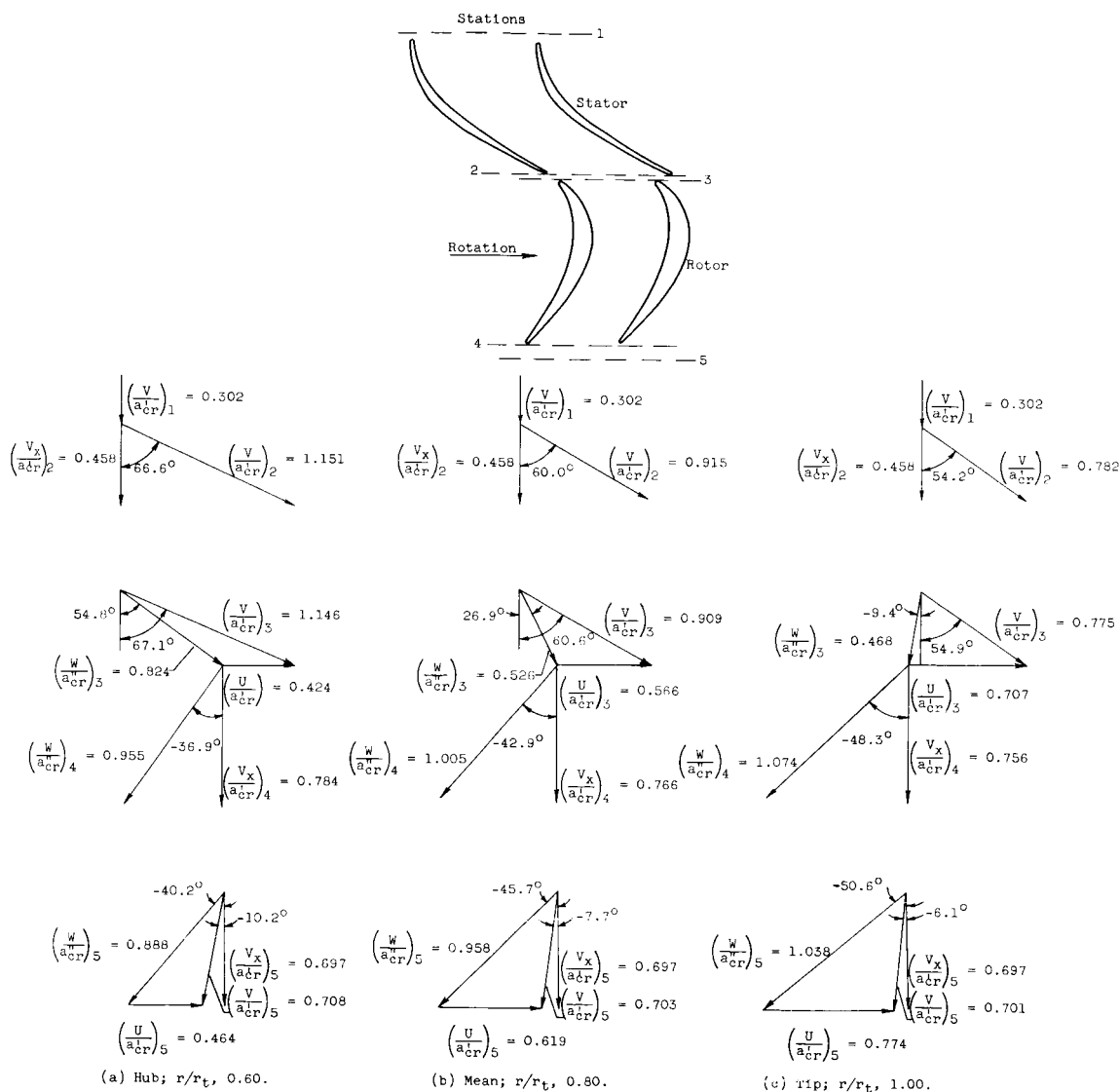


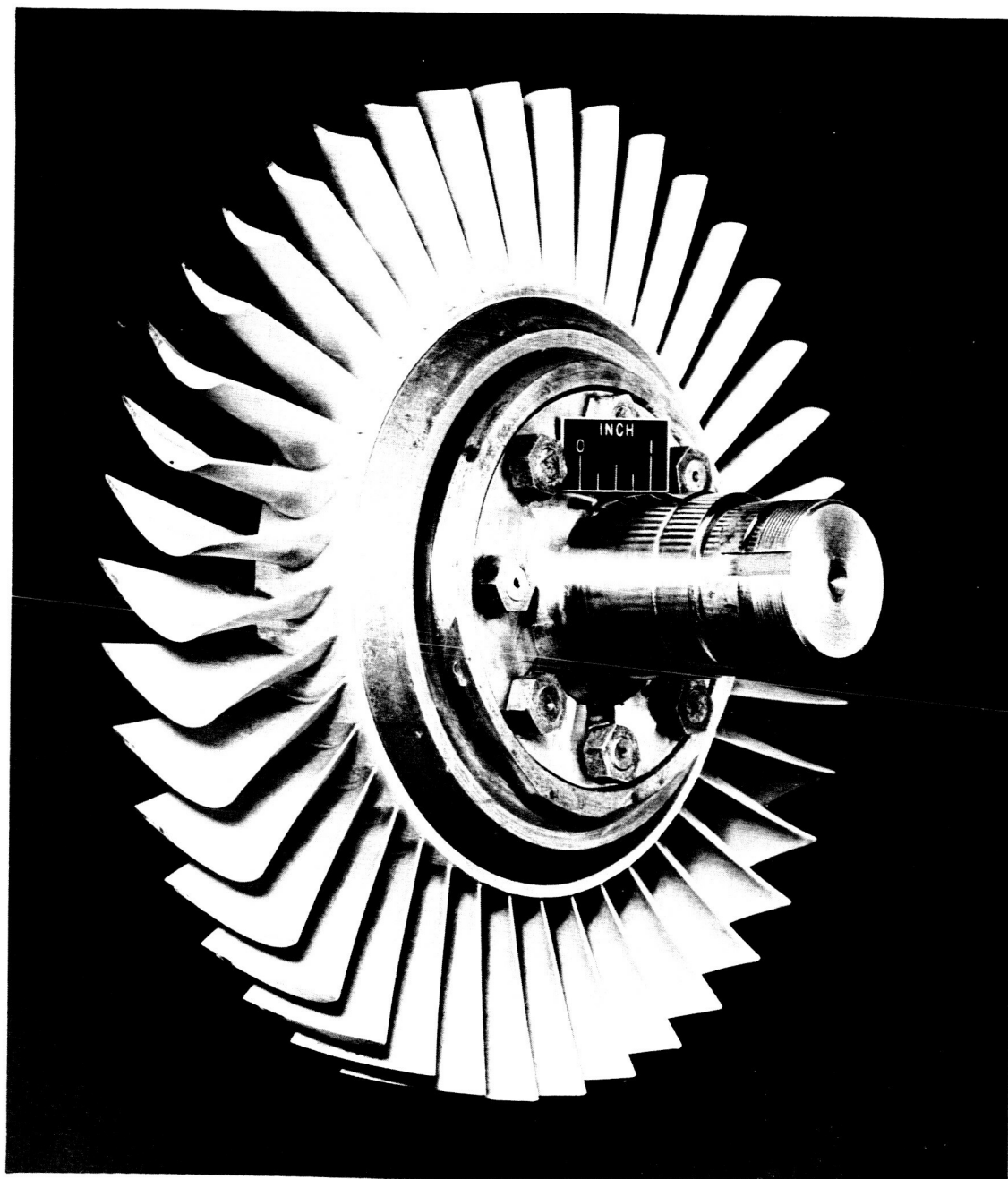
Figure 1. - Design velocity diagrams for subject turbine.

UNCLASSIFIED

NACA RM E56118

CONFIDENTIAL

13



C-41122

Figure 2. - Photograph of turbine rotor.

UNCLASSIFIED

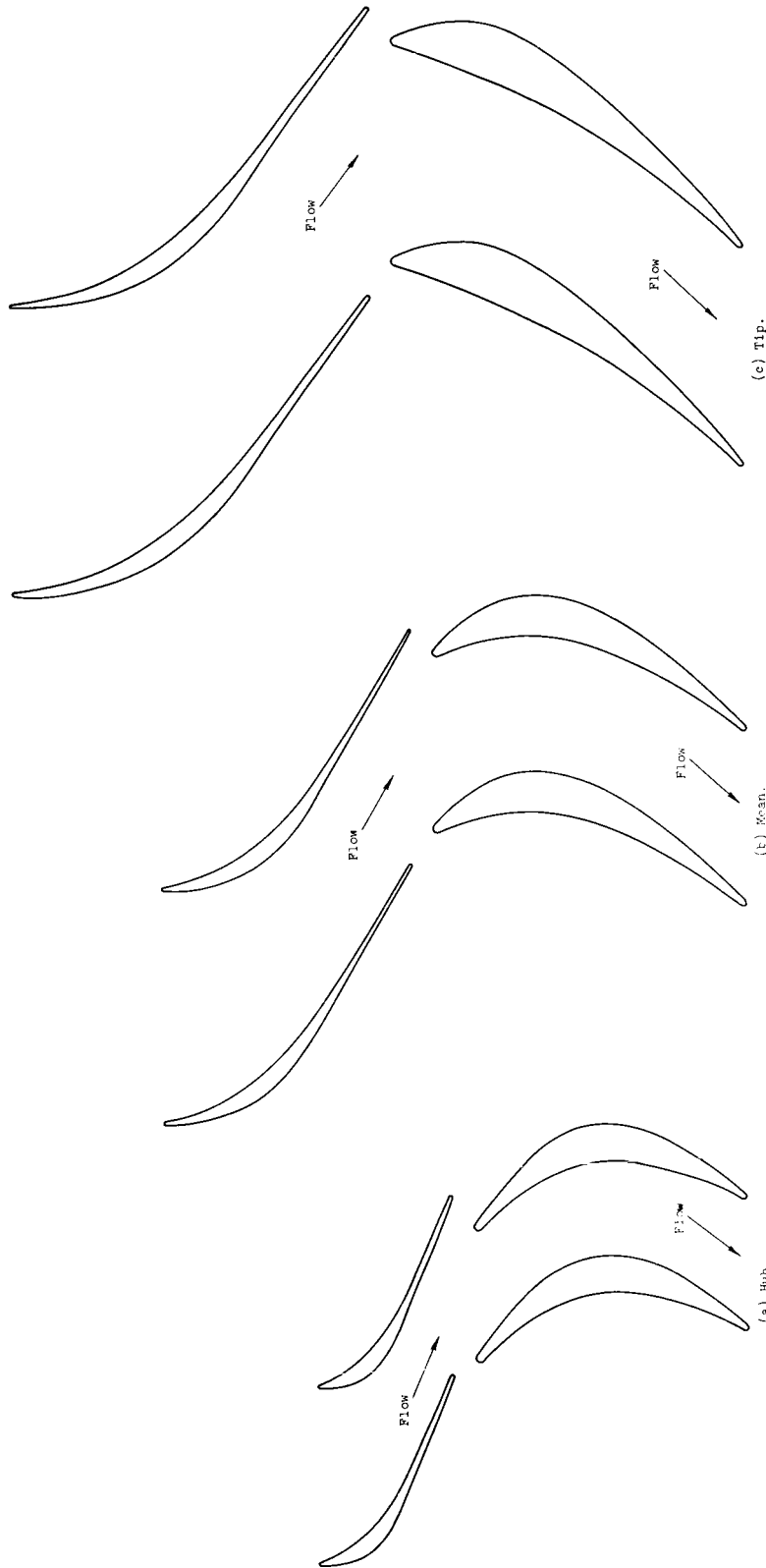


Figure 3. - Stator and rotor blade passages and profiles.

UNCLASSIFIED

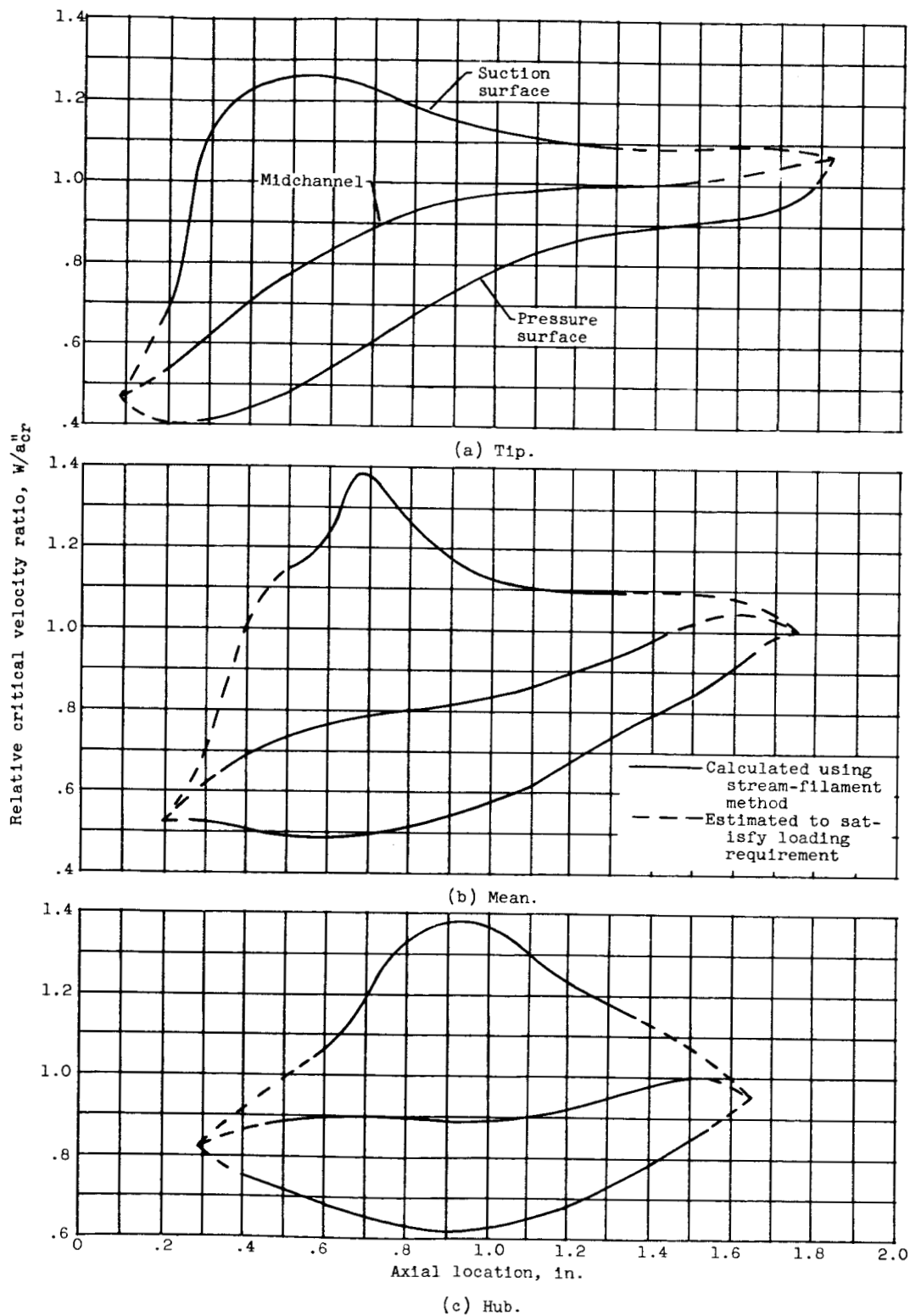
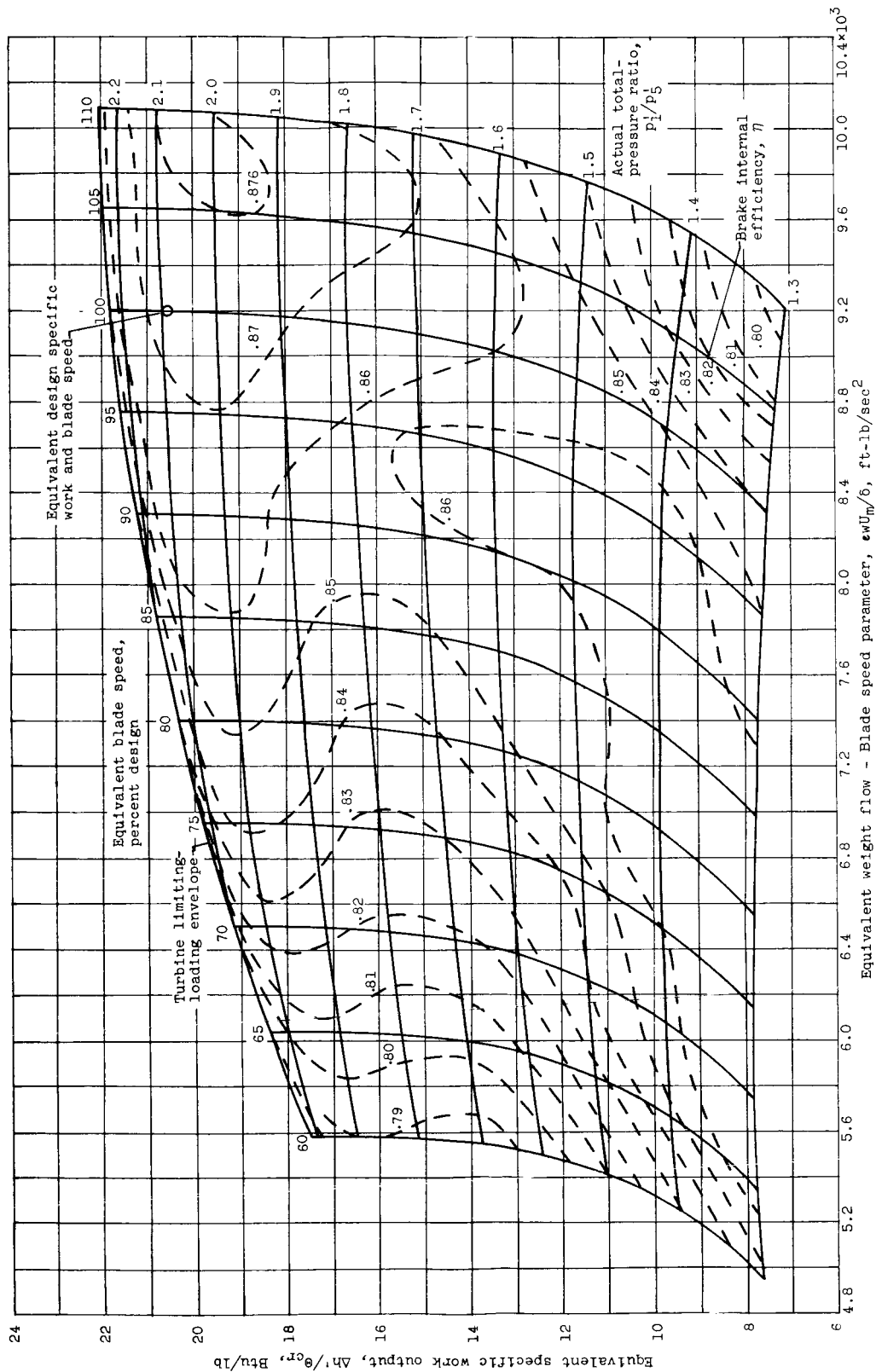


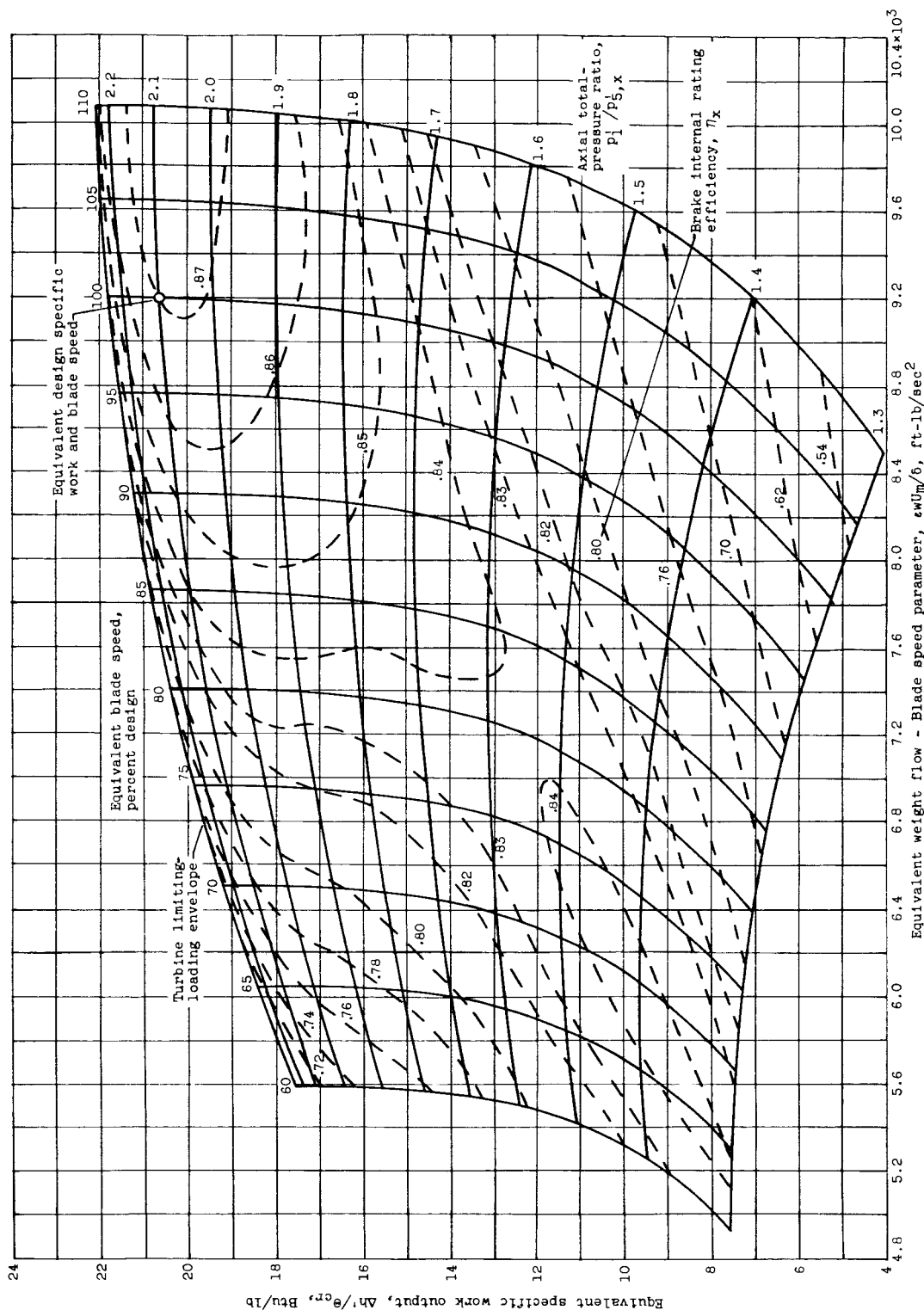
Figure 4. - Design rotor blade midchannel and surface velocity distributions at hub, mean, and tip sections.

UNCLASSIFIED



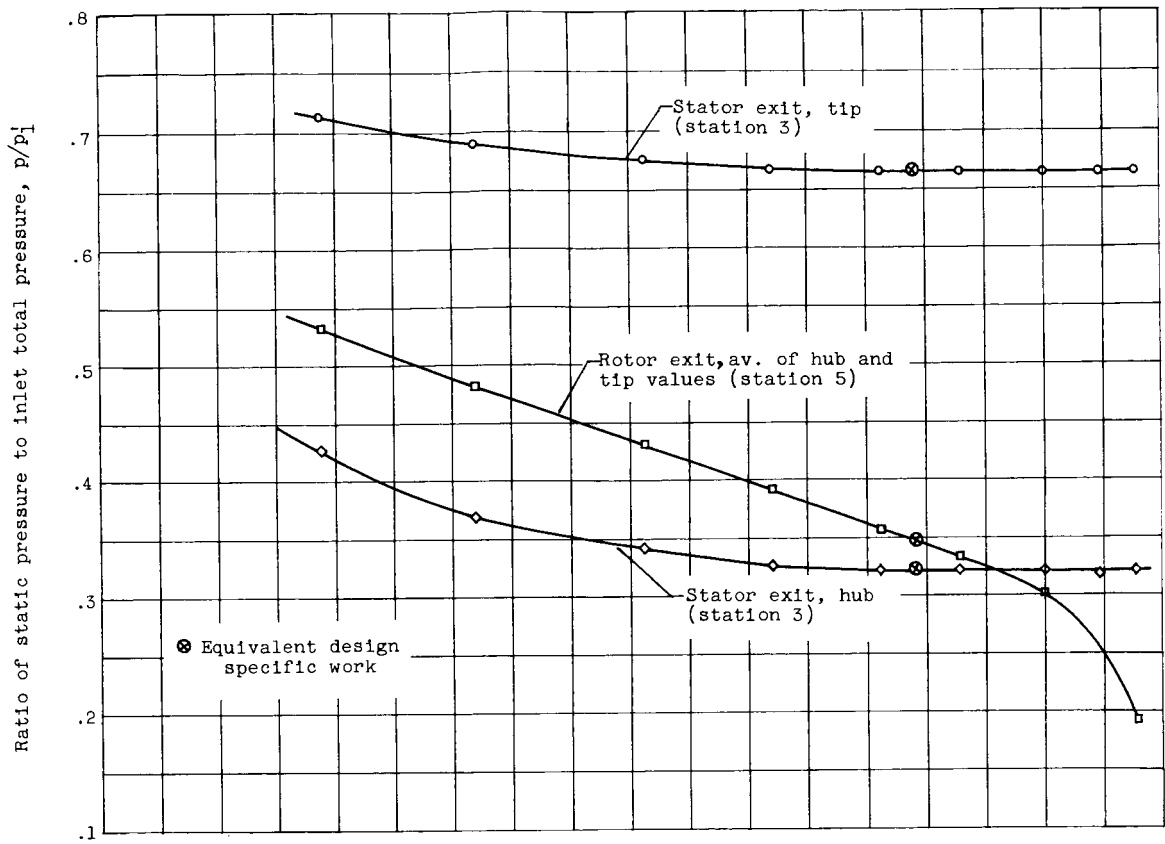
(a) Based on actual total-pressure ratio across turbine.

Figure 5. - Experimentally obtained turbine performance maps.

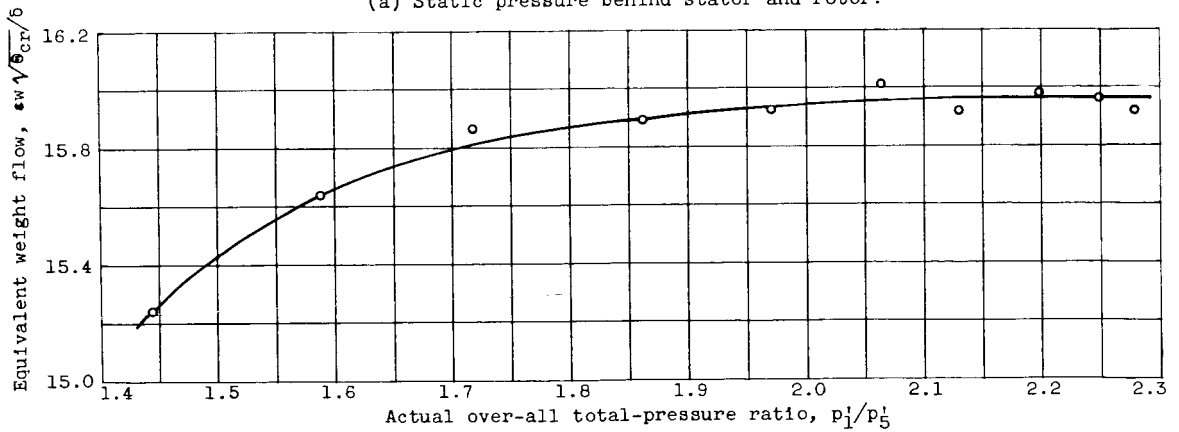


(b) Based on axial total-pressure ratio across turbine.

Figure 5. - Concluded. Experimentally obtained turbine performance maps.



(a) Static pressure behind stator and rotor.



(b) Equivalent weight flow.

Figure 6. - Variation of static pressure behind stator and rotor and equivalent weight flow with actual over-all total-pressure ratio at design speed.

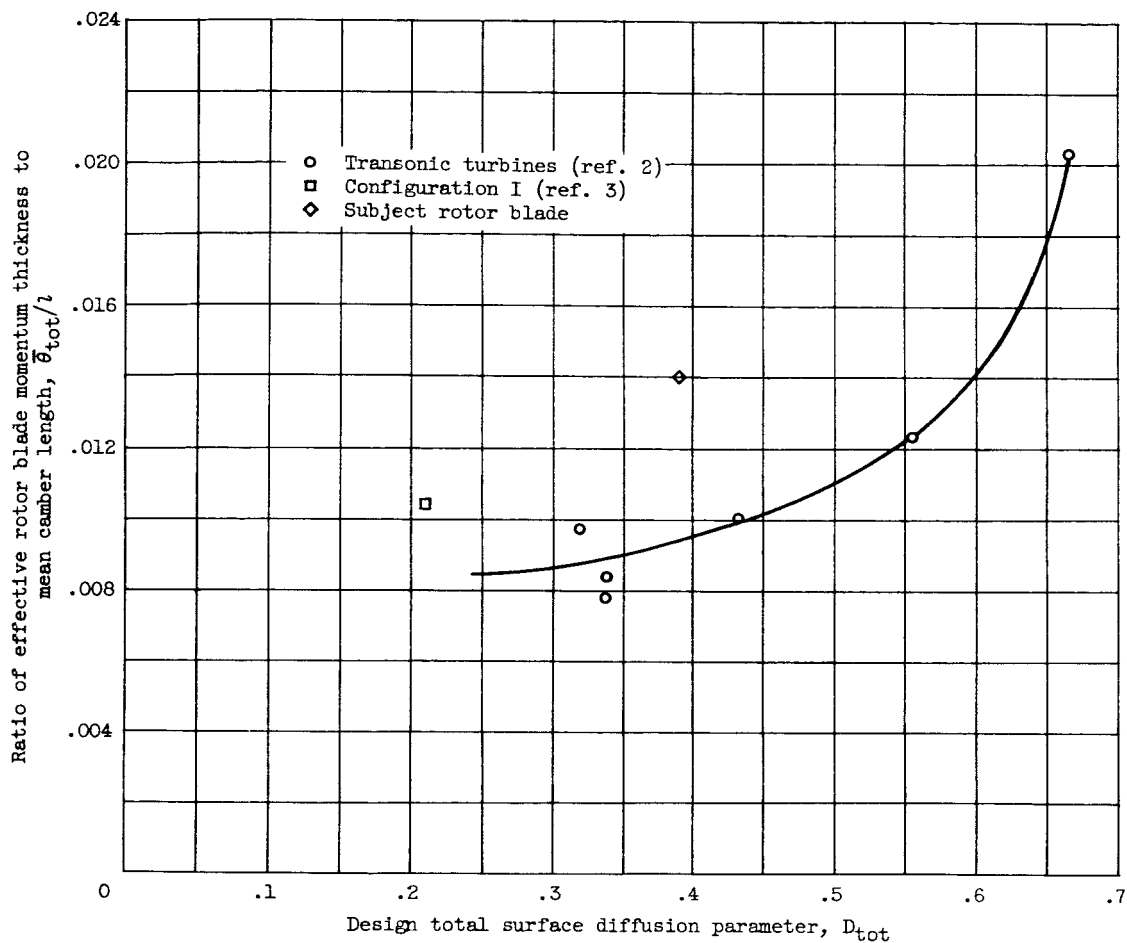


Figure 7. - Comparison of ratio of effective rotor blade momentum thickness to mean camber length of subject turbine with values for turbines of references 2 and 3.